Explicit-Form of Station-Keeping and Formation Flying Controller for Libration Point Orbits

Akiyama, Yuki
Department of Aeronautics and Astronautics, Kyushu University : Ph.D. Student

Bando, Mai
Department of Aeronautics and Astronautics, Kyushu University : Associate Professor

Hokamoto, Shinji
Department of Aeronautics and Astronautics, Kyushu University : Professor

出版情報：Journal of Guidance, Control, and Dynamics. 41 (6), pp.1407-1415, 2018-06. American Institute of Aeronautics and Astronautics (AIAA)
バージョン：
権利関係：

Explicit-Form of Station-Keeping and Formation Flying Controller for Libration Point Orbits

Yuki Akiyama[1], Mai Bando[2], and Shinji Hokamoto[3]
Kyushu University, Fukuoka 819-0385, Japan

I. Introduction

Recently unstable orbits in the vicinity of the libration points, or of the so-called Lagrangian points [1, 2], in the circular restricted three-body problem (CRTBP) have attracted much attention, and station-keeping on them has been studied by several authors [3–9]. For formation flying along unstable orbits, a simple feedback law was proposed by Scheeres [10] by stabilizing the unstable manifold and creating additional center manifolds. Based on the output regulation theory of a linear system [11], a control law to realize the formation flying and station-keeping was proposed by Bando and Ichikawa [12]. The periodic Riccati differential equations were used by Peng et al. for the station-keeping and formation flying based on the linear periodic time-varying equation of the relative motion around a libration point orbit [13].

In this paper, station-keeping and formation flying along unstable libration point orbits are considered. Using the nonlinear output regulation theory [14, 15], a general form of controller is analytically derived to achieve station-keeping and formation flying of periodic and quasi-periodic (invariant tori) orbits embedded on a four-dimensional center manifold in the CRTBP.

A standard approach to derive such a controller is to linearize the system along a reference orbit and then stabilize the linearized system [6, 16]. In our approach, the problem is solved as a nonlinear output regulation problem which allows us to derive a general form for station-keeping and formation flying controllers without the linearization assumption. However, the nonlinear output regulation problem cannot be applied directly to this problem due to an unstable mode. Therefore, by using the center manifold theory in the formulation

---

[1] Ph.D. Student, Department of Aeronautics and Astronautics, Kyushu University, akimaru@aero.kyushu-u.ac.jp.
[2] Associate Professor, Department of Aeronautics and Astronautics, Kyushu University, mbando@aero.kyushu-u.ac.jp. Member AIAA.
[3] Professor, Department of Aeronautics and Astronautics, Kyushu University, hokamoto@aero.kyushu-u.ac.jp. Member AIAA.

of the nonlinear output regulation problem, this paper proposes a station-keeping controller for a nonlinear reference orbit which can be solved explicitly when the initial condition of such a trajectory is assumed to be known exactly. Then, a Fourier series approximation is introduced to describe a periodic or quasi-periodic orbit in the CRTBP when the initial condition is not exactly known. By using the Fourier series approximation to describe a periodic or quasi-periodic orbit in the CRTBP, a neutrally stable exosystem to describe a reference trajectory for station-keeping is developed and the explicit solution to the nonlinear regulation problem is derived. However, it is nearly impossible to obtain the exact initial condition of a periodic orbit or quasi-periodic orbit. Thus, the proposed method based on a Fourier series approximation provides a practical controller to implement station-keeping or formation flying.

After describing the relevant theory and controller derivation, this paper presents numerical examples using the L_2 Lagrange point of the Sun-Earth CRTBP. For performance indexes, two velocity changes are calculated. Through the demonstrations of the transfer and station-keeping problem of the halo orbit, the relation between the truncation order and the performance indexes is revealed. As a further application, the result is applied to station-keeping and formation flying using artificial orbits. Furthermore, the controller is verified under realistic situations including various perturbations.

II. Equations of Motion in CRTBP

In the CRTBP, the equations of motion in the non-dimensional form [17] are expressed as

$$\begin{aligned} X'' - 2Y' &= \frac{\partial U}{\partial X} + u_x \\ Y'' + 2X' &= \frac{\partial U}{\partial Y} + u_y \\ Z'' &= \frac{\partial U}{\partial Z} + u_z \end{aligned} \tag{1}$$

where $\{X, Y, Z\}$ is the rotating frame whose origin is the barycenter of the system; the coordinates and time are normalized by the distance between the two main bodies and by the period of the circular orbit respectively; $(\cdot)'$ denotes the differentiation of $(\cdot)$ with respect to non-dimensional time t; (u_x, u_y, u_z) is the control acceleration;

$$
\begin{aligned}
U &= \frac{1-\mu}{r_1} + \frac{\mu}{r_2} + \frac{1}{2}\left(X^2+Y^2\right) \\
r_1 &= \sqrt{(X+\mu)^2+Y^2+Z^2} \\
r_2 &= \sqrt{(X-1+\mu)^2+Y^2+Z^2}
\end{aligned}
$$

and $\mu = M_2/(M_1+M_2)$ where M_1 and M_2 are the masses of the two main bodies with $M_1 > M_2$.

Equation (1) has libration points known as Lagrangian points L_i satisfying

$$
\frac{\partial U}{\partial X} = \frac{\partial U}{\partial Y} = \frac{\partial U}{\partial Z} = 0 \tag{2}
$$

and the Lagrangian points are expressed as

$$
\begin{aligned}
&L_1 = (l_1(\mu),0,0), \quad L_2 = (l_2(\mu),0,0), \quad L_3 = (l_3(\mu),0,0) \\
&L_4 = (1/2-\mu, \sqrt{3}/2, 0), \quad L_5 = (1/2-\mu, -\sqrt{3}/2, 0)
\end{aligned}
$$

where $l_i(\mu)$ are determined by setting $Y=0$ and solving $\dfrac{\partial U}{\partial X} = 0$. To describe the motion near a collinear libration point L_i ($i = 1,2,3$), it is convenient to use a coordinate system with the origin at L_i. Thus, replacing $\{X,Y,Z\}$ by $\{x+l_i, y, z\}$ and rewriting Eq. (1) in the state space form yield

$$
\boldsymbol{x}' = \boldsymbol{A}\boldsymbol{x} + \boldsymbol{B}\boldsymbol{f}(\boldsymbol{x}) + \boldsymbol{B}\boldsymbol{u} \tag{3}
$$

where $\boldsymbol{x} = \begin{bmatrix} x & y & z & x' & y' & z' \end{bmatrix}^{\mathrm{T}}$, $\boldsymbol{u} = \begin{bmatrix} u_x & u_y & u_z \end{bmatrix}^{\mathrm{T}}$, $\boldsymbol{B} = \begin{bmatrix} \boldsymbol{O}_3 & \boldsymbol{I}_3 \end{bmatrix}^{\mathrm{T}}$ and

$$
\boldsymbol{A} = \begin{bmatrix} \boldsymbol{O}_3 & \boldsymbol{I}_3 \\ \boldsymbol{K} & \boldsymbol{J} \end{bmatrix}, \ \boldsymbol{K} = \begin{bmatrix} 2\sigma_i+1 & 0 & 0 \\ 0 & 1-\sigma_i & 0 \\ 0 & 0 & -\sigma_i \end{bmatrix}, \ \boldsymbol{J} = \begin{bmatrix} 0 & 2 & 0 \\ -2 & 0 & 0 \\ 0 & 0 & 0 \end{bmatrix}
$$

$$
\boldsymbol{f}(\boldsymbol{x}) = \begin{bmatrix} \dfrac{\partial U}{\partial x} - (2\sigma_i+1)x \\ \dfrac{\partial U}{\partial y} - (1-\sigma_i)y \\ \dfrac{\partial U}{\partial z} + \sigma_i z \end{bmatrix}
$$

$$
\sigma_i = \frac{1-\mu}{|l_i(\mu)+\mu|^3} + \frac{\mu}{|l_i(\mu)-1+\mu|^3}
$$

Note that $\boldsymbol{f}(\boldsymbol{x})$ is the higher-order terms that would be dropped in the linearization.

III. Nonlinear Output Regulation Problem

The nonlinear output regulation theory is reviewed in this section. The detailed description is introduced in [14, 15]. The output regulation problem for a general nonlinear system is modeled by

$$\dot{\boldsymbol{x}} = \boldsymbol{f}(\boldsymbol{x}, \boldsymbol{u}, \boldsymbol{w}) \tag{4}$$

$$\boldsymbol{e} = \boldsymbol{h}(\boldsymbol{x}, \boldsymbol{u}, \boldsymbol{w}) \tag{5}$$

$$\dot{\boldsymbol{w}} = \boldsymbol{s}(\boldsymbol{w}) \tag{6}$$

where state $\boldsymbol{x} \in \mathbb{R}^n$, control input $\boldsymbol{u} \in \mathbb{R}^m$, exogenous signal $\boldsymbol{w} \in \mathbb{R}^q$, and regulated output $\boldsymbol{e} \in \mathbb{R}^r$. Equation (4) is a plant, and the exogenous signal $\boldsymbol{w}$ is generated by an external autonomous system (6), which is called an exosystem. Assume that $\boldsymbol{f} : \mathbb{R}^n \times \mathbb{R}^m \times \mathbb{R}^q \to \mathbb{R}^n$, $\boldsymbol{h} : \mathbb{R}^n \times \mathbb{R}^m \times \mathbb{R}^q \to \mathbb{R}^r$, and $\boldsymbol{s} : \mathbb{R}^q \to \mathbb{R}^q$ are at least twice continuously differentiable, and also that $\boldsymbol{f}(\boldsymbol{0}, \boldsymbol{0}, \boldsymbol{0}) = \boldsymbol{0}$, $\boldsymbol{h}(\boldsymbol{0}, \boldsymbol{0}, \boldsymbol{0}) = \boldsymbol{0}$, and $\boldsymbol{s}(\boldsymbol{0}) = \boldsymbol{0}$. Moreover, the plant (4) and the exosystem (6) satisfy the following assumptions: the pair $\left(\dfrac{\partial \boldsymbol{f}}{\partial \boldsymbol{x}}(\boldsymbol{0}, \boldsymbol{0}, \boldsymbol{0}), \dfrac{\partial \boldsymbol{f}}{\partial \boldsymbol{u}}(\boldsymbol{0}, \boldsymbol{0}, \boldsymbol{0})\right)$ is stabilizable and the exosystem (6) is neutrally stable, which are necessary conditions to solve the local output regulation problem.

The local output regulation problem is to find a stabilizing feedback control law such that $\boldsymbol{e} \to \boldsymbol{0}$ as time goes to infinity for any initial states in a vicinity sufficiently close to $(\boldsymbol{x}(0), \boldsymbol{w}(0)) = (\boldsymbol{0}, \boldsymbol{0})$. This local output regulation problem is solvable if and only if there exist mappings $\boldsymbol{\pi}(\boldsymbol{w})$ and $\boldsymbol{c}(\boldsymbol{w})$ with $\boldsymbol{\pi}(\boldsymbol{0}) = \boldsymbol{0}$ and $\boldsymbol{c}(\boldsymbol{0}) = \boldsymbol{0}$ which satisfy the conditions:

$$\frac{\partial \boldsymbol{\pi}(\boldsymbol{w})}{\partial \boldsymbol{w}} \boldsymbol{s}(\boldsymbol{w}) = \boldsymbol{f}(\boldsymbol{\pi}(\boldsymbol{w}), \boldsymbol{c}(\boldsymbol{w}), \boldsymbol{w}) \tag{7}$$

$$\boldsymbol{0} = \boldsymbol{h}(\boldsymbol{\pi}(\boldsymbol{w}), \boldsymbol{c}(\boldsymbol{w}), \boldsymbol{w}) \tag{8}$$

Then, an admissible feedback control law is given by

$$\boldsymbol{u} = -\boldsymbol{F}(\boldsymbol{x} - \boldsymbol{\pi}(\boldsymbol{w})) + \boldsymbol{c}(\boldsymbol{w}) \tag{9}$$

where $\boldsymbol{F}$ is an arbitrary matrix such that $\left(\dfrac{\partial \boldsymbol{f}}{\partial \boldsymbol{x}}(\boldsymbol{0}, \boldsymbol{0}, \boldsymbol{0}) - \dfrac{\partial \boldsymbol{f}}{\partial \boldsymbol{u}}(\boldsymbol{0}, \boldsymbol{0}, \boldsymbol{0})\boldsymbol{F}\right)$ is stable.

IV. Station-Keeping and Formation Flying Controller

In this section, a station-keeping and formation flying problem for reference orbits is formulated as a tracking problem. The problem is solved as a special case of the output regulation problem. Two types of exosystems generating reference orbits are considered and the corresponding controllers are derived.

A. Controller for Exact Tracking

For station-keeping, a simple feedback control $\boldsymbol{u} = -\boldsymbol{F}(\boldsymbol{x} - \boldsymbol{x}_{ref})$, where $\boldsymbol{x}_{ref}$ denotes a state of a reference orbit, is often used [7, 17]. First we show that the simple feedback control $\boldsymbol{u} = -\boldsymbol{F}(\boldsymbol{x} - \boldsymbol{x}_{ref})$ is a solution to the exact output tracking problem for a nonlinear reference trajectory.

The state $\boldsymbol{x}_{ref}$ of the reference orbit satisfies

$$\boldsymbol{x}'_{ref} = \boldsymbol{A}\boldsymbol{x}_{ref} + \boldsymbol{B}\boldsymbol{f}(\boldsymbol{x}_{ref}) \tag{10}$$

It should be noted that the nonlinear output regulation theory cannot be applied directly to this problem, because the matrix $\boldsymbol{A}$ has one unstable eigenvalue as well as one stable and four center eigenvalues, and thus, the assumption of the nonlinear output regulation problem does not hold. This paper, therefore, uses the center manifold theorem [18, 19] to reduce the six dimensional system into the four dimensional one which lies on the center manifold and is neutrally stable.

Equation (10) can be block-diagonalized by a transformation matrix $\boldsymbol{T}$ composed of eigenvectors of $\boldsymbol{A}$ into the following form:

$$\boldsymbol{w}' = \boldsymbol{P}\boldsymbol{w} + \boldsymbol{f}_c(\boldsymbol{w}, w_s, w_u) \tag{11}$$

$$w_s{}' = q w_s + f_s(\boldsymbol{w}, w_s, w_u) \tag{12}$$

$$w_u{}' = r w_u + f_u(\boldsymbol{w}, w_s, w_u) \tag{13}$$

where $\begin{bmatrix} \boldsymbol{w}^{\mathrm{T}} & w_s & w_u \end{bmatrix}^{\mathrm{T}} = \boldsymbol{T}^{-1}\boldsymbol{x}_{ref}$; $(\boldsymbol{w}, w_s, w_u) \in \mathbb{R}^4 \times \mathbb{R}^1 \times \mathbb{R}^1$; $\boldsymbol{P}$ is the 4×4 matrix whose eigenvalues have zero real parts, $q < 0$, and $r > 0$; the functions $\boldsymbol{f}_c : \mathbb{R}^6 \to \mathbb{R}^4$, and $f_s, f_u : \mathbb{R}^6 \to \mathbb{R}^1$ are zero at the origin and their first derivatives evaluated at the origin are also zero. Then, the reduced system on the center manifold [20] is given by

$$\boldsymbol{w}' = \boldsymbol{P}\boldsymbol{w} + \boldsymbol{f}_c(\boldsymbol{w}, w_s(\boldsymbol{w}), w_u(\boldsymbol{w})) \triangleq \boldsymbol{s}(\boldsymbol{w}) \tag{14}$$

$$\boldsymbol{w}(0) = \boldsymbol{w}_0 = [\boldsymbol{T}^{-1}\boldsymbol{x}_{ref}(0)]_{1:4} \tag{15}$$

where $\boldsymbol{s} : \mathbb{R}^4 \to \mathbb{R}^4$ and $[(\cdot)]_{i:j}$ signifies the i^{th} to j^{th} components of vector $(\cdot)$. Since the reduced system (14) is neutrally stable, it can be regarded as the exosystem for the reference periodic orbit. It should be noted that because the $\boldsymbol{w}$ is the state of the reduced system, $\boldsymbol{\tau}(\boldsymbol{w}) = \boldsymbol{T}\begin{bmatrix} \boldsymbol{w}^{\mathrm{T}} & w_s(\boldsymbol{w}) & w_u(\boldsymbol{w}) \end{bmatrix}^{\mathrm{T}} \in \mathbb{R}^6$ is the state restricted on the center manifold and satisfies

$$\boldsymbol{\tau}(\boldsymbol{w})' = \boldsymbol{A}\boldsymbol{\tau}(\boldsymbol{w}) + \boldsymbol{B}\boldsymbol{f}(\boldsymbol{\tau}(\boldsymbol{w})) \tag{16}$$

Then, the regulated output is expressed as

$$\boldsymbol{e} = \begin{pmatrix} x - x_{ref} \\ y - y_{ref} \\ z - z_{ref} \end{pmatrix} = \boldsymbol{C}\left(\boldsymbol{x} - \boldsymbol{\tau}(\boldsymbol{w})\right) \tag{17}$$

where $\boldsymbol{C} = \begin{bmatrix} \boldsymbol{I}_3 & \boldsymbol{O}_3 \end{bmatrix}$. For Eqs. (3), (14) and (17), the mappings $\boldsymbol{\pi}(\boldsymbol{w})$ and $\boldsymbol{c}(\boldsymbol{w})$, which satisfy the conditions (7), and (8), are given by

$$\boldsymbol{\pi}(\boldsymbol{w}) = \boldsymbol{\tau}(\boldsymbol{w}) \tag{18}$$

$$\boldsymbol{c}(\boldsymbol{w}) = \boldsymbol{0} \tag{19}$$

Note that it is confirmed that Eqs. (18) and (19) are the solutions to the regulator equations because $\dfrac{\partial \boldsymbol{\pi}}{\partial \boldsymbol{w}}\boldsymbol{s}(\boldsymbol{w}) = \dfrac{\partial \boldsymbol{\tau}}{\partial \boldsymbol{w}}\boldsymbol{w}' = \boldsymbol{\tau}'(\boldsymbol{w})$ and Eq. (16).

Then, the controller to achieve asymptotic tracking is

$$\boldsymbol{u} = -\boldsymbol{F}(\boldsymbol{x} - \boldsymbol{\tau}(\boldsymbol{w})) = -\boldsymbol{F}(\boldsymbol{x} - \boldsymbol{x}_{ref}) \tag{20}$$

where $\boldsymbol{F}$ is an arbitrary feedback gain matrix such that $\boldsymbol{A} - \boldsymbol{B}\boldsymbol{F}$ is stable. Thus, the nonlinear output regulation theory can be applied to the station-keeping problem by introducing the center manifold theory. Moreover, mappings can be obtained explicitly, and consequently, the controller is given in the simple feedback form. It should be noted that though the proposed controller (20) is a simple linear feedback controller, it can achieve exact tracking to the nonlinear reference orbit.

B. Exosystem for Approximated Reference Orbit and Controller

The controller for a natural periodic orbit has been derived in the previous subsection. However, note that since the initial condition $\boldsymbol{x}_{ref}(0)$ is only numerically available, the orbit departing from the obtained $\boldsymbol{x}_{ref}(0)$ diverges within a few periods. Moreover, the controller (20) cannot deal with a formation flying problem since a formation flying orbit no longer satisfies Eq. (10).

This paper designs a neutrally stable exosystem and derives a general controller which is applicable for both station-keeping and formation flying by using a reference orbit approximated by a Fourier series. Let $\boldsymbol{x}_{ref}$ and $\boldsymbol{x}_{ref,n}$ be a state of a target orbit and the n^{th}-order approximation of $\boldsymbol{x}_{ref}$, respectively. The position vector of $\boldsymbol{x}_{ref,n}$ is given by

$$
\begin{aligned}
x_{ref,n}(t) &= a_{x0} + \sum_{k=1}^{n} (a_{xk} \cos k\omega_x t + b_{xk} \sin k\omega_x t) \\
y_{ref,n}(t) &= a_{y0} + \sum_{k=1}^{n} (a_{yk} \cos k\omega_y t + b_{yk} \sin k\omega_y t) \\
z_{ref,n}(t) &= a_{z0} + \sum_{k=1}^{n} (a_{zk} \cos k\omega_z t + b_{zk} \sin k\omega_z t)
\end{aligned}
\tag{21}
$$

where ω_x, ω_y, and ω_z are frequencies of the (quasi-) periodic reference orbit along each coordinate. In general these frequencies are not the same values, thereby, Eq. (21) represents a quasi-periodic orbit. As a special case of $\omega_x = \omega_y = \omega_z$, Eq. (21) becomes a periodic orbit.

The exosystem generating the n^{th}-order approximated reference orbit described by Eq. (21) is expressed as a linear state space form:

$$
\boldsymbol{w}_n' = \boldsymbol{S}_n \boldsymbol{w}_n, \;\; \boldsymbol{w}_n(0) = \boldsymbol{w}_0 \tag{22}
$$

where $\boldsymbol{w}_n = \begin{bmatrix} \boldsymbol{w}_{x,n}^{\mathrm{T}} & \boldsymbol{w}_{y,n}^{\mathrm{T}} & \boldsymbol{w}_{z,n}^{\mathrm{T}} \end{bmatrix}^{\mathrm{T}}$; $\boldsymbol{w}_{x,n}, \boldsymbol{w}_{y,n}, \boldsymbol{w}_{z,n} \in \mathbb{R}^{2n+1}$; $\boldsymbol{w}_0 = \begin{bmatrix} \boldsymbol{w}_{x0}^{\mathrm{T}} & \boldsymbol{w}_{y0}^{\mathrm{T}} & \boldsymbol{w}_{z0}^{\mathrm{T}} \end{bmatrix}^{\mathrm{T}}$; $\boldsymbol{S}_n = \mathrm{diag}\begin{bmatrix} \boldsymbol{S}_{x,n} & \boldsymbol{S}_{y,n} & \boldsymbol{S}_{z,n} \end{bmatrix}$; $\boldsymbol{S}_{j,n} = \mathrm{diag}\begin{bmatrix} 0 & \boldsymbol{D}_{j,1} & \boldsymbol{D}_{j,2} & \cdots & \boldsymbol{D}_{j,n} \end{bmatrix} \in \mathbb{R}^{(2n+1)\times(2n+1)}$;

$$
\begin{aligned}
\boldsymbol{w}_{j,n} &= \left[\begin{array}{c|cc|cc|c|cc} w_{j,0} & w_{j,1} & \bar{w}_{j,1} & w_{j,2} & \bar{w}_{j,2} & \cdots & w_{j,n} & \bar{w}_{j,n} \end{array}\right]^{\mathrm{T}} \\
\boldsymbol{w}_{j0} &= \left[\begin{array}{c|cc|cc|c|cc} a_{j0} & a_{j1} & b_{j1} & a_{j2} & b_{j2} & \cdots & a_{jn} & b_{jn} \end{array}\right]^{\mathrm{T}} \\
\boldsymbol{D}_{j,n} &= \begin{bmatrix} 0 & n\omega_j \\ -n\omega_j & 0 \end{bmatrix}, \quad (j = x, y, z)
\end{aligned}
$$

Then, the solutions to Eq. (22) are given by

$$
\begin{aligned}
w_{j,0}(t) &= a_{j0} \\
w_{j,n}(t) &= a_{jn} \cos n\omega_j t + b_{jn} \sin n\omega_j t \\
\bar{w}_{j,n}(t) &= -a_{jn} \sin n\omega_j t + b_{jn} \cos n\omega_j t
\end{aligned}
\tag{23}
$$

Hence, the reference orbit Eq. (21) is expressed as the superposition of the first and second equations of

Eq. (23) as

$$
\begin{aligned}
x_{ref,n}(t) &= \sum_{k=0}^{n} w_{x,k} = \boldsymbol{L}\boldsymbol{w}_{x,n}, \\
y_{ref,n}(t) &= \sum_{k=0}^{n} w_{y,k} = \boldsymbol{L}\boldsymbol{w}_{y,n}, \\
z_{ref,n}(t) &= \sum_{k=0}^{n} w_{z,k} = \boldsymbol{L}\boldsymbol{w}_{z,n}
\end{aligned}
\tag{24}
$$

where $\boldsymbol{L} = \left[\begin{array}{c|cc|cc|c|cc} 1 & 1 & 0 & 1 & 0 & \cdots & 1 & 0 \end{array}\right]$.

The regulated output is defined as

$$
\boldsymbol{e} = \begin{pmatrix} x - x_{ref,n} \\ y - y_{ref,n} \\ z - z_{ref,n} \end{pmatrix} = \boldsymbol{C}\boldsymbol{x} - \boldsymbol{D}\boldsymbol{w}_n \tag{25}
$$

with $\boldsymbol{D} = \mathrm{diag}[\boldsymbol{L}, \boldsymbol{L}, \boldsymbol{L}]$. For Eqs. (3), (22) and (25), the mappings $\boldsymbol{\pi}_n(\boldsymbol{w}_n)$ and $\boldsymbol{c}_n(\boldsymbol{w}_n)$, which satisfy the conditions (7), and (8), are given by

$$
\boldsymbol{\pi}_n(\boldsymbol{w}_n) = \begin{bmatrix} \boldsymbol{D} \\ \boldsymbol{D}\boldsymbol{S}_n \end{bmatrix} \boldsymbol{w}_n \triangleq \boldsymbol{\Pi}_n \boldsymbol{w}_n \tag{26}
$$

$$
\boldsymbol{c}_n(\boldsymbol{w}_n) = -\boldsymbol{f}(\boldsymbol{\Pi}_n\boldsymbol{w}_n) + (\boldsymbol{D}\boldsymbol{S}_n^2 - \boldsymbol{K}\boldsymbol{D} - \boldsymbol{J}\boldsymbol{D}\boldsymbol{S}_n)\boldsymbol{w}_n \triangleq -\boldsymbol{f}(\boldsymbol{\Pi}_n\boldsymbol{w}_n) + \boldsymbol{\Gamma}_n\boldsymbol{w}_n \tag{27}
$$

Note that the regulator equations are nonlinear but have explicit solutions (26) and (27) since the designed exosystem is linear.

Then, the controller for the n^{th}-order problem to achieve asymptotic tracking is obtained as

$$
\boldsymbol{u}_n = -\boldsymbol{F}(\boldsymbol{x} - \boldsymbol{\Pi}_n\boldsymbol{w}_n) - \boldsymbol{f}(\boldsymbol{\Pi}_n\boldsymbol{w}_n) + \boldsymbol{\Gamma}_n\boldsymbol{w}_n \tag{28}
$$

where $\boldsymbol{u}$ has been replaced by $\boldsymbol{u}_n$ in order to clarify the dependence on the truncation order. By applying the feedback control (28), the state $\boldsymbol{x}$ asymptotically tracks the reference orbit $\boldsymbol{x}_{ref,n}$ for any $(\boldsymbol{x}(0), \boldsymbol{w}(0))$ and stays in the vicinity of it. When the reference orbit is exactly periodic, the control cost for station-keeping evaluated in the absolute integral, *i.e.* L_1 norm, can be made arbitrarily small for sufficient large truncation order of Fourier series. However, in practice, L_1 norm does not exactly converge to zero because of the small numerical error in the initial condition. Further, the discontinuities of the reference orbit at $t = 0, T$ might lead an unexpected overshoot of control input at the discontinuity called Gibbs phenomenon. To avoid this, the reference orbit must be modified to be a continuous periodic orbit. By using a interpolating technique, the order of the L_1 norm for sufficiently large n and t is the same as that of the sum of the maximum error between the states of the reference discontinuous trajectory and the interpolated orbit and that between the interpolated orbit and the natural periodic orbit (see Appendix A).

Comparing the controller (28) with the controller (20), the controller (28) requires not only a feedback term but also additional terms to achieve tracking due to the approximation of the reference orbit. However, the controller (28) is the n^{th}-order approximation of the controller (20), and both controllers accord for a sufficiently large truncation order (see Appendix B). The proposed control law (28) realizes station-keeping on a periodic orbit which is free motion in the considered system with few control input. Moreover, if a reference orbit is not free motion in the system, the proposed control law (28) can achieve station-keeping on an artificial orbit.

V. Simulation Results for Sun-Earth CRTBP

In this section, the control law (28) is applied to the nonlinear equations of motion (1) around the L_2 Lagrange point of the Sun-Earth CRTBP. First, station-keeping on a halo orbit is considered to verify the developed controller. Then, formation flying along the halo orbit is demonstrated as a further application. Furthermore, the effects of perturbations on the performance of the controller is investigated. The period of the orbit and the radius of the Sun-Earth system are assumed to be $T_0 = 365.26$ days and $R_0 = 1.4960 \times 10^8$ km, respectively. Then, the parameters are specified as $\mu = 3.0542 \times 10^{-6}$, $l_2 = 1.0101$, and $\sigma_2 = 3.9393$. The initial condition for the halo orbit in the normalized units is given by

$$\boldsymbol{x}_{ref}(0) = \begin{bmatrix} -2.2556 & 0 & 2.2901 & 0 & 11.721 & 0 \end{bmatrix} \times 10^{-3} \tag{29}$$

and its period is $T = 3.0934$ (179.70 days).

A. Station-Keeping on Libration Orbits

Note that the trajectory with the initial condition (29) is not exactly periodic, and that it diverges within four periods. First, the trajectory is interpolated to be a continuous periodic orbit by setting $\boldsymbol{x}_{ref}(T) = \boldsymbol{x}_{ref}(0)$. Then, to represent the interpolated reference orbit in analytical form, the time history of the position of the orbit during the first period is expanded in the n^{th}-order Fourier series. The n^{th}-order reference orbit,

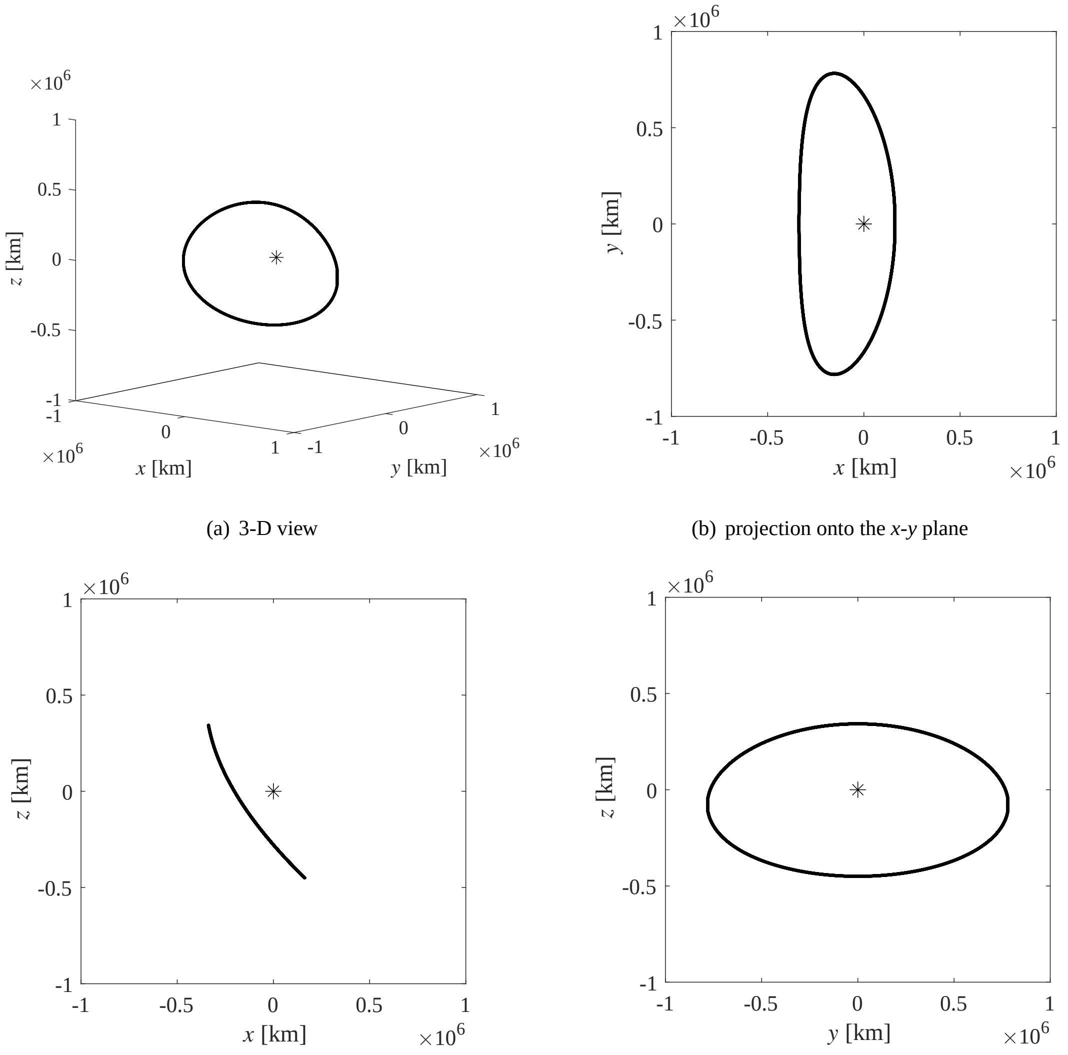

(a) 3-D view (b) projection onto the *x*-*y* plane

(c) projection onto the *x*-*z* plane (d) projection onto the *y*-*z* plane

Fig. 1 Pseudo-periodic orbit ($n = 8$).

referred to as *pseudo-periodic orbit*, is shown in Fig. 1. The initial condition obtained for the pseudo-periodic orbit $\boldsymbol{x}_{ref,8}(0)$ is slightly different from Eq. (29) due to the truncation error of Fourier series.

As a preliminary step, the feedback gain $\boldsymbol{F}$ is designed by the linear quadratic regulator (LQR) theory and is given by $\boldsymbol{F} = \boldsymbol{R}^{-1}\boldsymbol{B}^{\mathrm{T}}\boldsymbol{X}$, where $\boldsymbol{X}$ is the solution to the algebraic Ricatti equation

$$\boldsymbol{A}^{\mathrm{T}}\boldsymbol{X} + \boldsymbol{X}\boldsymbol{A} + \boldsymbol{Q} - \boldsymbol{X}\boldsymbol{B}\boldsymbol{R}^{-1}\boldsymbol{B}^{\mathrm{T}}\boldsymbol{X} = \boldsymbol{0}$$

where $\boldsymbol{Q} = \boldsymbol{I}_6$ and $\boldsymbol{R} = \boldsymbol{I}_3$.

A state that is slightly different from the stable manifold of the halo orbit is used as the initial state of

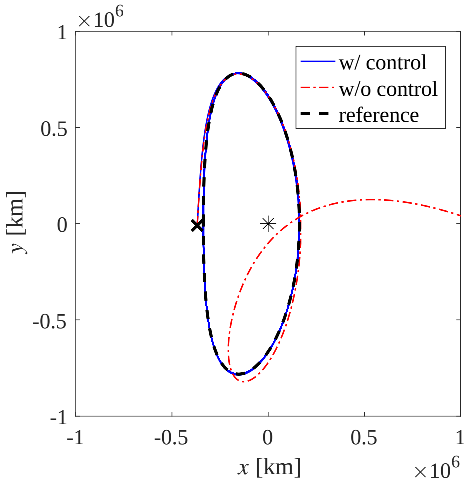

(a) projection onto the x-y plane

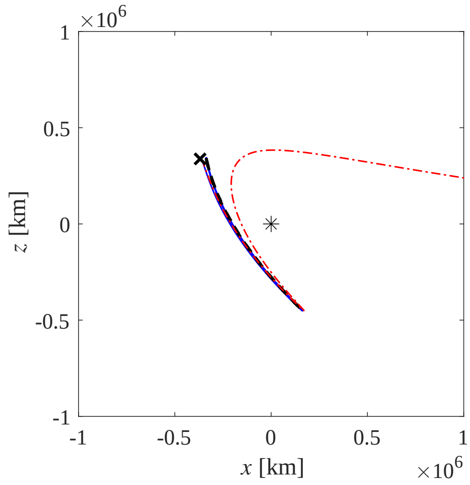

(b) projection onto the x-z plane

Fig. 2 Controlled trajectory ($n = 8$); the solid and chain lines are the controlled and uncontrolled trajectories, respectively, and the dashed line is the reference orbit.

the spacecraft. The state on the stable manifold given by

$$\boldsymbol{x}_{stable} = \begin{bmatrix} -2.4671 & -0.061698 & 2.2600 & 0.68730 & 12.131 & 0.036903 \end{bmatrix} \times 10^{-3} \tag{30}$$

converges to the halo orbit after approximately 510 days without control. Then, the initial state $\boldsymbol{x}_0$ that includes the position errors $(300\text{km}, -100\text{km}, 200\text{km})$ for $\boldsymbol{x}_{stable}$ as

$$\boldsymbol{x}_0 = \begin{bmatrix} -2.4651 & -0.062367 & 2.2587 & 0.68730 & 12.131 & 0.036903 \end{bmatrix} \times 10^{-3} \tag{31}$$

is used for the simulation. Note that the trajectory departing from $\boldsymbol{x}_0$ diverges within one period without control. The initial state of the exosystem $\boldsymbol{w}_0$ is set using the Fourier coefficients and frequencies for $n = 8$.

The controlled trajectory by Eq. (28) is shown in Fig. 2, and the time history of the control input and its enlargement are shown in Fig. 3. Figure 2 shows that the state asymptotically tracks the pseudo-periodic orbit. It can be seen from Fig. 3 that the input gets smaller as time passes and becomes periodic. This is because the state $\boldsymbol{x}$ approaches $\boldsymbol{\Pi}_n \boldsymbol{w}_n = \boldsymbol{x}_{ref,n}$ and the input $\boldsymbol{u}$ converges to $(-\boldsymbol{f}(\boldsymbol{\Pi}_n \boldsymbol{w}_n) + \boldsymbol{\Gamma}_n \boldsymbol{w}_n)$ as $t \to \infty$.

Two performance indexes are considered: ΔV_0 and ΔV_1. The definition of ΔV_0 is the absolute integral, *i.e.* L_1 norm, of the input until the time T_{conv} when the distance from the reference trajectory δ becomes smaller than a specific value ε. Another index, ΔV_1, is defined as the L_1 norm of the input for one-period

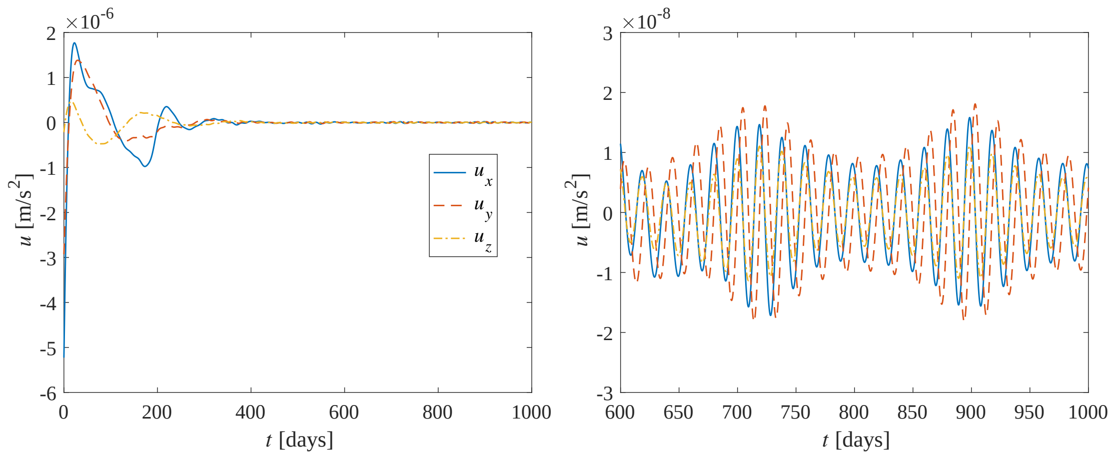

(a) input (b) enlargement

Fig. 3 Time history of input ($n = 8$).

after time T_{conv}. That is,

$$\Delta V_0 = \int_0^{T_{conv}} |\boldsymbol{u}_n(t)|dt = \int_0^{T_{conv}} |u_x(t)| + |u_y(t)| + |u_z(t)|dt \tag{32}$$

$$\Delta V_1 = \int_{T_{conv}}^{T_{conv}+T} |\boldsymbol{u}_n(t)|dt = \int_{T_{conv}}^{T_{conv}+T} |u_x(t)| + |u_y(t)| + |u_z(t)|dt \tag{33}$$

Here, ΔV_0 and ΔV_1 are calculated as a function of the truncation order n and shown in Fig. 4 for $n = 3, 4, \cdots, 8$, for $\varepsilon = 6.6846 \times 10^{-8}$ (corresponding to 10 km). Figure 4(a) shows that ΔV_0 approaches the specific value (31.859 m/s) as n increases. From Fig. 4(b), ΔV_1 approaches zero. This is because the higher-order approximation generates a closer orbit to the reference orbit that is sufficiently close to a natural periodic orbit, and hence, control effort for station-keeping approaches zero. However, in practice, ΔV_1 does not converges to zero but converges to a small value (in this example, ΔV_1 goes to 0.18522 m/s) because the reference orbit is not free motion.

B. Formation Flying using Quasi-Periodic Orbits

The derived controller applies to a general form of tracking problem, and formation flying can be achieved by changing the parameters in the controller. Consider a chief satellite orbiting a reference halo orbit generated by the initial condition (29) and a deputy satellite which is to fly in formation with the chief. As an example, a circular formation flying orbit in the x-y plane is considered. By changing (a_{xk}, b_{yk}) to $(a_{xk} + r, b_{yk} + r)$ where k is the index of the Fourier series, the relative motion of the deputy with respect to

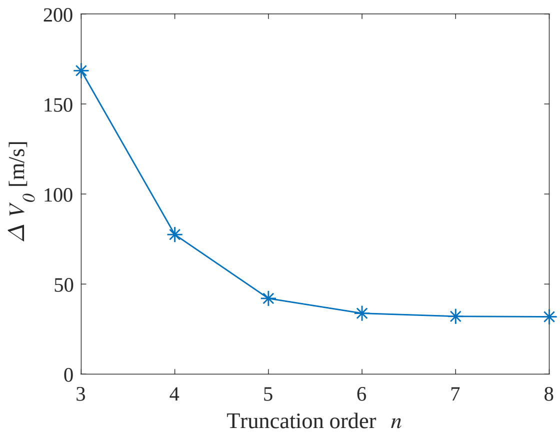

(a) ΔV_0 and n

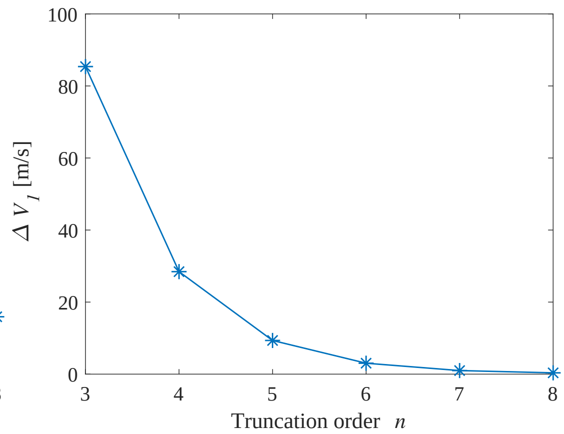

(b) ΔV_1 and n

Fig. 4 Relation between performance indexes and *n*.

the chief $\delta\boldsymbol{r} = \begin{bmatrix} \delta x & \delta y & \delta z \end{bmatrix}^{\mathrm{T}}$ become a circular orbit in the *x*-*y* plane whose radius is r as

$$\begin{aligned} \delta x(t) &= r\cos k\omega_x t \\ \delta y(t) &= r\sin k\omega_y t \\ \delta z(t) &= 0 \end{aligned} \tag{34}$$

Note that while the chief rotates one revolution, the deputy does k revolutions around the chief. The truncation order of the halo orbit and formation flying orbits is $n = 8$. To exaggerate the formation flying orbits, the radius is set as $r = 2.0054 \times 10^{-4}$ (30,000 km) in the simulation. The formation flying orbits for $k = 2$ and 8 are shown in Fig. 5. When $r = 2.0054 \times 10^{-6}$ (300 km), the maintenance cost for the formation flying for one period is 6.8918 m/s for $k = 2$ and 70.633 m/s for $k = 8$.

C. Effects of Perturbations on the Proposed Controller

In this subsection, the effects of the perturbations, including the solar radiation pressure (SRP), modeling error, process noise, and measurement error, on the performance of the derived controller (28) are considered. Assume as follows: (i) the spacecraft is always perpendicular to the sun direction, *i.e.* the SRP acceleration $\boldsymbol{a}_{SRP}$ is oriented along the radial direction, (ii) the process noise is represented by $\boldsymbol{d}_f \in \mathbb{R}^3$ and each component of $\boldsymbol{d}_f$ has the normal distribution $(0, \sigma_f^2)$, (iii) the measurement error about the position is represented by $\boldsymbol{d}_p \in \mathbb{R}^3$ and each component of $\boldsymbol{d}_p$ has the normal distribution $(0, \sigma_p^2)$, and (iv) the measurement error about the velocity is represented by $\boldsymbol{d}_v \in \mathbb{R}^3$ and each component of $\boldsymbol{d}_v$ has the normal distribution $(0, \sigma_v^2)$.

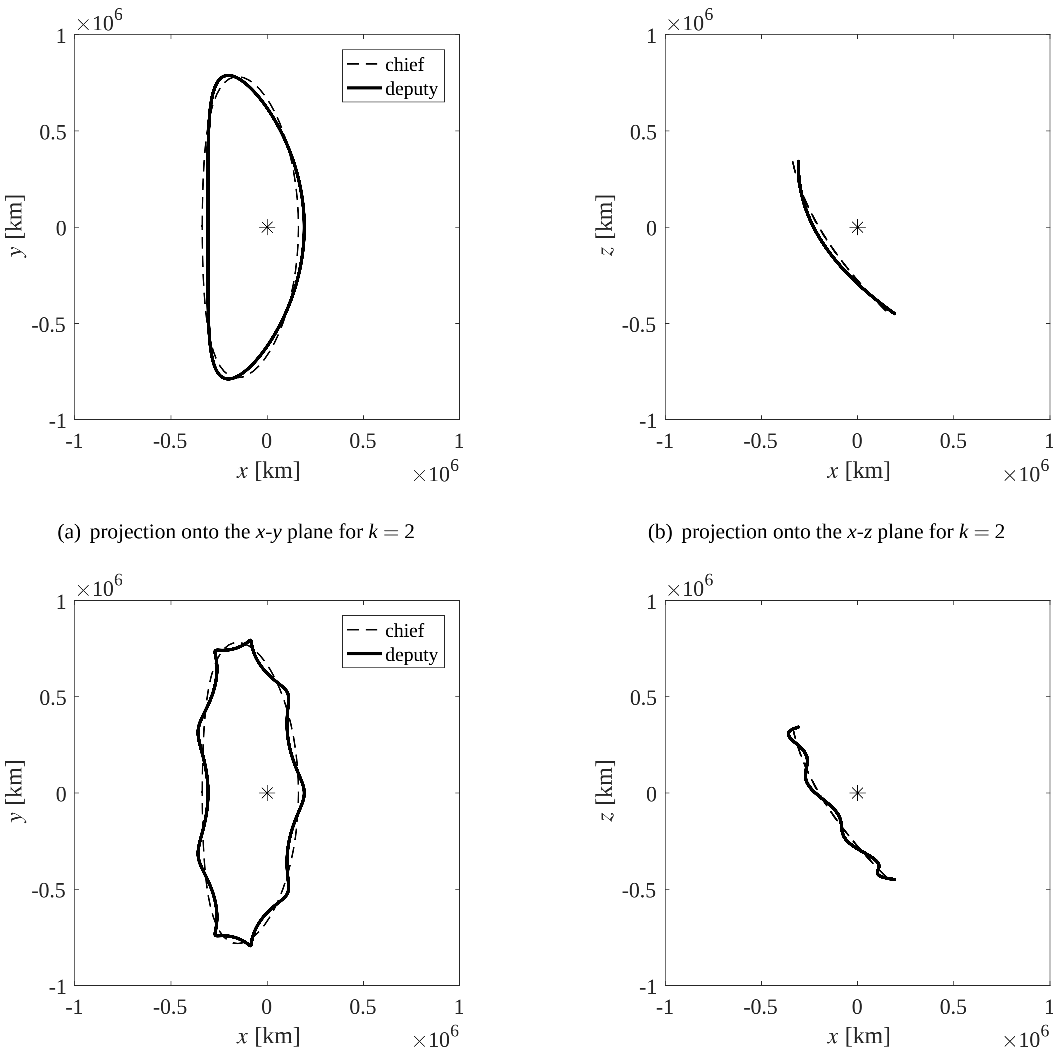

(a) projection onto the x-y plane for $k = 2$

(b) projection onto the x-z plane for $k = 2$

(c) projection onto the x-y plane for $k = 8$

(d) projection onto the x-z plane for $k = 8$

Fig. 5 Formation flying orbits ($n = 8$); the dashed and solid lines are orbits of the chief and the deputy, respectively.

Then, the CRTBP including the SRP and the process noise is expressed by

$$\boldsymbol{x}' = \boldsymbol{A}\boldsymbol{x} + \boldsymbol{B}\boldsymbol{f}(\boldsymbol{x}) + \boldsymbol{B}\boldsymbol{u} + \boldsymbol{B}\boldsymbol{a}_{SRP} + \boldsymbol{B}\boldsymbol{d}_f \tag{35}$$

The SRP acceleration is computed by

$$\boldsymbol{a}_{SRP}(\boldsymbol{x};\beta) = \beta \frac{1-\mu}{r_1^3} \boldsymbol{r}_1 \tag{36}$$

and β is the lightness number, defined as the ratio of the SRP acceleration to solar gravitational acceleration.

To investigate the effects of the perturbations to the control performance, station-keeping on the halo orbit obtained by the initial condition (29) is considered where the controller (28) is applied to the disturbed model (35). The initial state of the spacecraft is set as Eq. (31), and the initial state of the exosystem $\boldsymbol{w}_0$ is set using the Fourier coefficients and frequencies for $n = 8$. Further, the parameters are set as $\beta = 0.005$, $\sigma_f = 1.5 \times 10^{-3}$ mm/s^2, $\sigma_p = 10$ km, and $\sigma_f = 10$ m/s.

The controlled trajectory by Eq. (28) and the time history of the control input are shown in Fig. 6. Due to the perturbations, the spacecraft does not converge to the reference orbit exactly but converges to the deviated periodic orbit (Fig. 6(a)), and the control input also does not approaches zero but becomes almost periodic (Fig. 6(b)).

The controller for dealing with the SRP can be easily derived as the extension of the controller (28) because the model of the perturbation is explicitly given. The modified controller including the measurement error is obtained as

$$\boldsymbol{u}_n = -\boldsymbol{F}(\boldsymbol{x} - \boldsymbol{\Pi}_n \boldsymbol{w}_n) - \boldsymbol{f}(\boldsymbol{\Pi}_n \boldsymbol{w}_n) - \boldsymbol{a}(\boldsymbol{\Pi}_n \boldsymbol{w}_n; \hat{\beta}) + \boldsymbol{\Gamma}_n \boldsymbol{w}_n \tag{37}$$

where $\hat{\beta}$ denotes the lightness number including the estimation error of β. The modified controller (37) is applied to the disturbed model model (35). All the conditions are the same as those for Fig. 6, and $\hat{\beta}$ is set as $\hat{\beta} = 1.1\beta$.

The controlled trajectory by Eq. (37) and the time history of the control input are shown in Fig. 7. Although the small error exists, the spacecraft almost converges to the reference orbit in Fig. 7(a). Further, the control input in Fig. 7(b) is smaller than that in Fig. 6(b) because the modified controller can deal with the effect of the SRP.

VI. Conclusion

A new station-keeping strategy based on nonlinear output regulation theory has been proposed for the periodic orbits in the circular restricted three-body problem. A Fourier series approximation was employed to generate the desired orbits, and then, the output regulation theory for nonlinear systems was applied. The output regulation problem was solved in an analytical form. The proposed controller has been applied and verified in numerical simulations for the halo orbit of the Sun-Earth L_2 point. In the case that the reference orbit is the natural periodic orbit, the controller can approximate the optimal controller in the sense of minimizing the station-keeping cost. As an application of the proposed method, formation flying using circular orbits around the chief satellite have been worked out. In our framework, solving a various formation problem is equivalent to solving an output regulation problem with suitable parameters. Furthermore, the effects

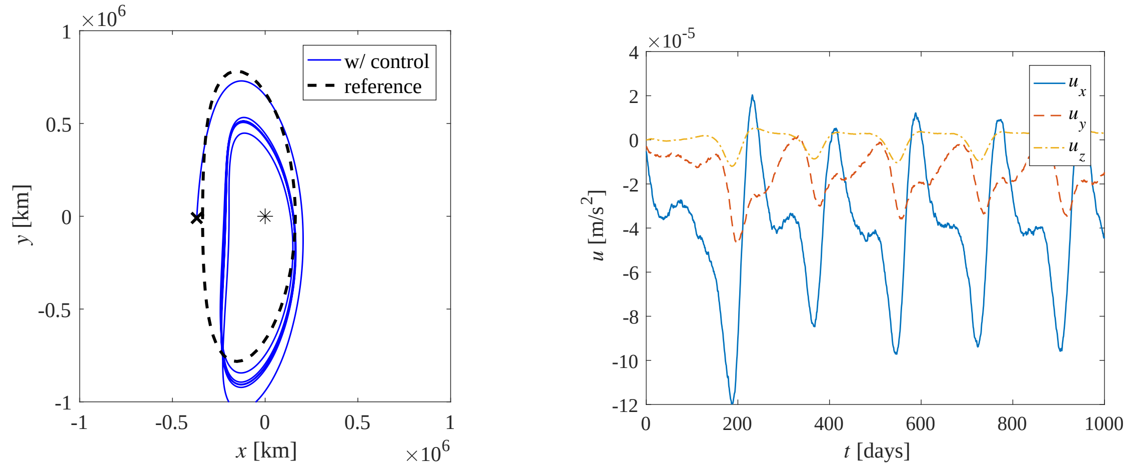

(a) projection onto the x-y plane (b) input

Fig. 6 Simulation results using the controller (28)**; (a) the solid line is the controlled trajectories and the dashed line is the reference orbit; (b) time history of input.**

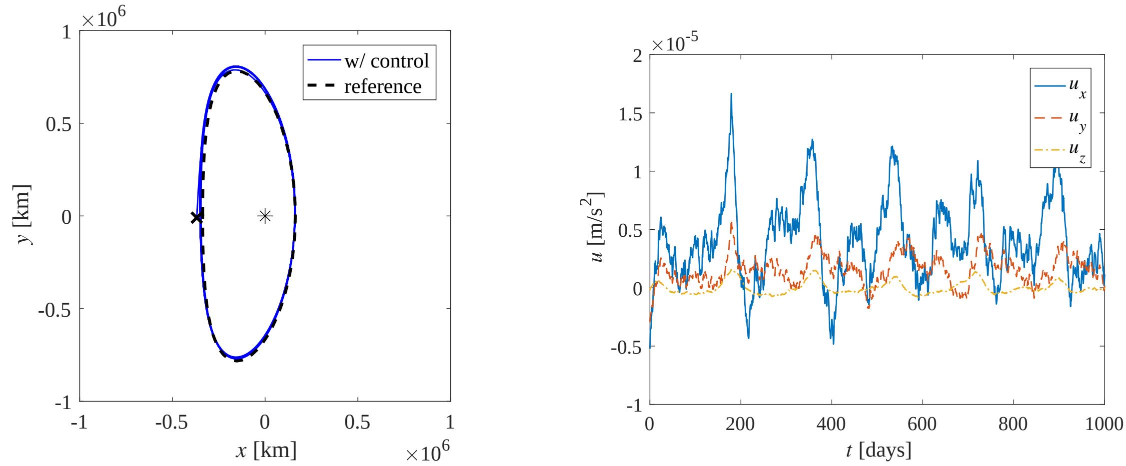

(a) projection onto the x-y plane (b) input

Fig. 7 Simulation results using the controller (37)**; (a) the solid line is the controlled trajectories and the dashed line is the reference orbit; (b) time history of input.**

of the perturbations, including the solar radiation pressure, modeling error, process noise, and measurement noise, on the performance of the proposed controller have been investigated. Then, the modified controller has been proposed and verified. The proposed control strategy is applicable to both station-keeping and formation flying and easy to implement in practical situations.

Appendix

A. Relation between truncation order and total control input

Let assume as follows: (i) $\boldsymbol{x}_{ref}$ is a state of an exact periodic orbit whose period is T, and the initial state is given by $\boldsymbol{x}_{ref}(0)$, (ii) $\hat{\boldsymbol{x}}_{ref}$ is a state of a reference trajectory defined on the interval $[0,T]$ and the initial state is given by $\hat{\boldsymbol{x}}_{ref}(0)$ that are slightly different from $\boldsymbol{x}_{ref}(0)$, (iii) $\tilde{\boldsymbol{x}}_{ref}$ is a state of a periodic function defined by interpolating $\hat{\boldsymbol{x}}_{ref}$ such that $\hat{\boldsymbol{x}}_{ref}(T) = \hat{\boldsymbol{x}}_{ref}(0)$, where the initial state is given by $\tilde{\boldsymbol{x}}_{ref}(0) = \hat{\boldsymbol{x}}_{ref}(0)$, (iv) $\tilde{\boldsymbol{x}}_{ref,n}$ is the n^{th}-order Fourier approximation of $\tilde{\boldsymbol{x}}_{ref}$, where the initial condition is given by $\tilde{\boldsymbol{x}}_{ref,n}(0) = \tilde{\boldsymbol{x}}_{ref}(0)$, (v) $\delta\boldsymbol{x}_n = \tilde{\boldsymbol{x}}_{ref,n} - \boldsymbol{x}_{ref}$ is the difference between the states of the n^{th}-order approximation of the reference orbit and the exact periodic orbit, where its period is T.

First, it is shown that $|\delta\boldsymbol{x}_n(t)|$ becomes equal to or less than a specific value by choosing sufficiently large n and t. From the inequality

$$|\delta\boldsymbol{x}_n(t)| \le |\tilde{\boldsymbol{x}}_{ref,n}(t) - \tilde{\boldsymbol{x}}_{ref}(t)| + |\tilde{\boldsymbol{x}}_{ref}(t) - \hat{\boldsymbol{x}}_{ref}(t)| + |\hat{\boldsymbol{x}}_{ref}(t) - \boldsymbol{x}_{ref}(t)| \tag{38}$$

$|\delta\boldsymbol{x}_n(t)| \le h_1 + h_2 = h$ for sufficiently large n and t, where

$$h_1 = \max_{t\in[t',t'+T]} |\tilde{\boldsymbol{x}}_{ref}(t) - \hat{\boldsymbol{x}}_{ref}(t)| \tag{39}$$

$$h_2 = \max_{t\in[t',t'+T]} |\hat{\boldsymbol{x}}_{ref}(t) - \boldsymbol{x}_{ref}(t)| \tag{40}$$

Next, it is shown that the order of the performance index $\Delta V_1 = \int_t^{t+T} |\boldsymbol{u}_n(t)| dt = \int_t^{t+T} |u_x(t)| + |u_y(t)| + |u_z(t)| dt$ is the same as that of h and h' for sufficiently large n and t, where $h' = h_1' + h_2'$,

$$h_1' = \max_{t\in[t',t'+T]} |\tilde{\boldsymbol{x}}_{ref}'(t) - \hat{\boldsymbol{x}}_{ref}'(t)| \tag{41}$$

$$h_2' = \max_{t\in[t',t'+T]} |\hat{\boldsymbol{x}}_{ref}'(t) - \boldsymbol{x}_{ref}'(t)| \tag{42}$$

The regulated output is given by

$$\boldsymbol{e} = \boldsymbol{C}(\boldsymbol{x} - \tilde{\boldsymbol{x}}_{ref,n}) \tag{43}$$

Therefore, the convergence of $\boldsymbol{e}$ to zero implies $|\boldsymbol{x}(t) - \tilde{\boldsymbol{x}}_{ref,n}| \to 0$ as $t \to \infty$. Further, from the facts $\boldsymbol{\Pi}_n \boldsymbol{w}_n = \tilde{\boldsymbol{x}}_{ref,n}$ and $\boldsymbol{\Gamma}_n \boldsymbol{w}_n = \boldsymbol{B}^{\mathrm{T}}(\tilde{\boldsymbol{x}}_{ref,n}' - \boldsymbol{A}\tilde{\boldsymbol{x}}_{ref,n})$, Eq.(26) can be deformed as

$$\begin{aligned}\boldsymbol{u}_n &= -\boldsymbol{F}(\boldsymbol{x} - \tilde{\boldsymbol{x}}_{ref,n}) - \boldsymbol{f}(\tilde{\boldsymbol{x}}_{ref,n}) + \boldsymbol{B}^{\mathrm{T}}\left(\tilde{\boldsymbol{x}}_{ref,n}' - \boldsymbol{A}\tilde{\boldsymbol{x}}_{ref,n}\right) \\ &= -\boldsymbol{F}(\boldsymbol{x} - \tilde{\boldsymbol{x}}_{ref,n}) - \frac{\partial \boldsymbol{f}}{\partial \boldsymbol{x}}(\boldsymbol{x}_{ref})\delta\boldsymbol{x}_n + \boldsymbol{B}^{\mathrm{T}}\left(\delta\boldsymbol{x}_n' - \boldsymbol{A}\delta\boldsymbol{x}_n\right) + O(\delta\boldsymbol{x}_n^2)\end{aligned} \tag{44}$$

Then from the inequality

$$|\boldsymbol{u}_n| \le \|\boldsymbol{F}\||\boldsymbol{x}-\tilde{\boldsymbol{x}}_{ref,n}| + |\delta\boldsymbol{x}'_n| + \left[\left\|\frac{\partial \boldsymbol{f}}{\partial \boldsymbol{x}}(\boldsymbol{x}_{ref})\right\| + \|\boldsymbol{A}\|\right]|\delta\boldsymbol{x}_n| + O(\delta\boldsymbol{x}_n^2) \tag{45}$$

and neglecting the higher-order term

$$|\boldsymbol{u}_n(t)| \le h' + \left[\left\|\frac{\partial \boldsymbol{f}}{\partial \boldsymbol{x}}(\boldsymbol{x}_{ref})\right\| + \|\boldsymbol{A}\|\right] h \tag{46}$$

for sufficiently large n and t, where $\|(\cdot)\|$ denotes the matrix norm of $(\cdot)$ and $\|\boldsymbol{B}^{\mathrm{T}}\| = 1$ is used. Thus, the maximum of the performance index for sufficiently large n and t' is

$$\Delta V_1 = \int_{t'}^{t'+T} |\boldsymbol{u}_n(t)| dt \le \max_{t\in[t',t'+T]} |\boldsymbol{u}_n(t)| T = \left(h' + \left[\left\|\frac{\partial \boldsymbol{f}}{\partial \boldsymbol{x}}(\boldsymbol{x}_{ref})\right\| + \|\boldsymbol{A}\|\right] h\right) T \tag{47}$$

From this analysis, the order of the performance index for sufficiently large n and t is the same as that of h and h'. Note that when the reference orbit is periodic, *i.e.* $\boldsymbol{x}_{ref} = \hat{\boldsymbol{x}}_{ref} = \tilde{\boldsymbol{x}}_{ref}$, $h = h' = 0$ and consequently, $\Delta V_1 = 0$ for sufficiently large n and t.

B. Relation between the controllers (20) and (28)

It is shown that the controller (28) is the n^{th}-order approximation of the controller (20). The controller (28) can be expressed as

$$\boldsymbol{u}_n = -\boldsymbol{F}(\boldsymbol{x}-\boldsymbol{x}_{ref,n}) - \boldsymbol{f}(\boldsymbol{x}_{ref,n}) + \boldsymbol{B}^{\mathrm{T}}\left(\boldsymbol{x}'_{ref,n} - \boldsymbol{A}\boldsymbol{x}_{ref,n}\right) \tag{48}$$

From a standard result of functional analysis [21], $\|\boldsymbol{x}_{ref} - \boldsymbol{x}_{ref,n}\| \to 0$ as n increases, where $\|\cdot\|$ denotes the uniform norm over one period. The variation of the controllers (20) and (28) can be deformed as

$$\boldsymbol{u} - \boldsymbol{u}_n = -\boldsymbol{F}(\boldsymbol{x}_{ref,n} - \boldsymbol{x}_{ref}) + \left(\boldsymbol{f}(\boldsymbol{x}_{ref,n}) - \boldsymbol{f}(\boldsymbol{x}_{ref})\right) - \boldsymbol{B}^{\mathrm{T}}\left\{(\boldsymbol{x}'_{ref,n} - \boldsymbol{x}'_{ref}) - \boldsymbol{A}(\boldsymbol{x}_{ref,n} - \boldsymbol{x}_{ref})\right\} \tag{49}$$

Then

$$|\boldsymbol{u} - \boldsymbol{u}_n| \le \|\boldsymbol{F}\||\boldsymbol{x}_{ref,n} - \boldsymbol{x}_{ref}| + |\boldsymbol{f}(\boldsymbol{x}_{ref,n}) - \boldsymbol{f}(\boldsymbol{x}_{ref})| + |\boldsymbol{x}'_{ref,n} - \boldsymbol{x}'_{ref}| + \|\boldsymbol{A}\||\boldsymbol{x}_{ref,n} - \boldsymbol{x}_{ref}| \tag{50}$$

Observe that $\boldsymbol{f}(\boldsymbol{x})$ is a continuous function of $\boldsymbol{x}$, and therefore, $|\boldsymbol{u} - \boldsymbol{u}_n| \to 0$ as $|\boldsymbol{x}_{ref} - \boldsymbol{x}_{ref,n}| \to 0$. That is, two controllers accord for a sufficiently large n.

References

[1] Howell, K. C., “Three-Dimensional, Periodic, ‘Halo’ Orbits,” *Celestial Mechanics*, Vol. 32, No. 1, 1984, pp. 53–71. doi:10.1007/BF01358403.

[2] Howell, K. C., “Families of Orbits in the Vicinity of the Collinear Libration Points,” *Journal of the Astronautical Sciences*, Vol. 49, No. 1, 2001, pp. 107–126.

[3] Dunham, D. W. and Roberts, C. E., “Stationkeeping Techniques for Libration-Point Satellites,” *The Journal of the astronautical sciences*, Vol. 49, No. 1, 2001, pp. 127–144.

[4] Breakwell, J. V., Kamel, A. A., and Ratner, M. J., “Station-Keeping for a Translunar Communication Station,” *Celestial Mechanics*, Vol. 10, No. 3, September 1974, pp. 357–373. doi:10.1007/bf01586864.

[5] Simó, C., Gómez, G., Llibre, J., Martinez, R., and Rodriguez, J., “On the Optimal Station Keeping Control of Halo Orbits,” *Acta Astronautica*, Vol. 15, No. 6-7, June 1987, pp. 391–397. doi:10.1016/0094-5765(87)90175-5.

[6] Howell, K. C. and Pernicka, H. J., “Station-Keeping Method for Libration Point Trajectories,” *Journal of Guidance, Control, and Dynamics*, Vol. 16, No. 1, January 1993, pp. 151–159. doi:10.2514/3.11440.

[7] Gómez, G., Jorba, A., Llibre, J., Martínez, R., and Simó, C., *Dynamics and Mission Design Near Libration Points: Volume I: Fundamentals: The Case of Collinear Libration Points*, Vol. 2, World Scientific, 2001.

[8] Folta, D. C., Pavlak, T. A., Haapala, A. F., Howell, K. C., and Woodard, M. A., “Earth–Moon Libration Point Orbit Stationkeeping: Theory, Modeling, and Operations,” *Acta Astronautica*, Vol. 94, No. 1, January 2014, pp. 421–433. doi:10.1016/j.actaastro.2013.01.022.

[9] Ardaens, J.-S. and D’Amico, S., “Control of Formation Flying Spacecraft at a Lagrange Point,” *DLR Technical Note*, , No. 00-08, January 2008.

[10] Scheeres, D. J., Hsiao, F.-Y., and Vinh, N. X., “Stabilizing Motion Relative to an Unstable Orbit: Applications to Spacecraft Formation Flight,” *Journal of Guidance, Control, and Dynamics*, Vol. 26, No. 1, January 2003, pp. 62–73. doi:10.2514/2.5015.

[11] Saberi, A., Sannuti, P., and Stoorvogel, A., *Control of Linear Systems with Regulation and Input Constraints*, Springer-Verlag, Berlin, 2000, pp. 13–68.

[12] Bando, M. and Ichikawa, A., “Formation Flying Along Halo Orbit of Circular-Restricted Three-Body Problem,” *Journal of Guidance, Control, and Dynamics*, Vol. 38, No. 1, January 2015, pp. 123–129. doi:10.2514/1.g000463.

[13] Peng, H., Zhao, J., Wu, Z., and Zhong, W., “Optimal Periodic Controller for Formation Flying on Libration Point Orbits,” *Acta Astronautica*, Vol. 69, No. 7, 2011, pp. 537–550. doi:10.1016/j.actaastro.2011.04.020.

[14] Isidori, A. and Byrnes, C. I., “Output Regulation of Nonlinear Systems,” *IEEE Transactions on Automatic Control*, Vol. 35, No. 2, 1990, pp. 131–140. doi:10.1109/9.45168.

[15] Suzuki, H., Sakamoto, N., and Celikovskỳ, S., “Analytical Approximation Method for the Center Manifold in the

Nonlinear Output Regulation Problem," *47th IEEE Conference on Decision and Control*, Institute of Electrical and Electronics Engineers, 2008, pp. 1163–1168. doi:10.1109/CDC.2008.4738935.

[16] Folta, D. and Vaughn, F., "A Survey of Earth-Moon Libration Orbits: Stationkeeping Strategies and Intra-Orbit Transfers," August 2004. doi:10.2514/6.2004-4741.

[17] Wie, B., *Space Vehicle Dynamics and Control*, AIAA Education Series, Reston, VA, 1998.

[18] Khalil, H. K., *Nonlinear Systems*, Prentice Hall, New Jewsey, 3rd ed., 2002.

[19] Perko, L., *Differential Equations and Dynamical Systems*, Springer-Verlag, New York, 3rd ed., 2001.

[20] Akiyama, Y., Bando, M., Hamidreza, N., and Hokamoto, S., "Trajectory design using the center manifold theory in the circular restricted three-body problem," *Transactions of the Japan Society for Aeronautical and Space Sciences, Aerospace Technology Japan*, Vol. 14, No. ists30, 2016, pp. Pd_151–Pd_158.

[21] Hanna, J. R. and John, H. R., *Fourier Series, Transforms, and Boundary Value Problems*, John Wiley & Sons, New York, 2nd ed., 1990, pp. 68–101.